ELSEVIER

Nuclear Physics A631 (1998) 353c–362c

NUCLEAR PHYSICS A

Precision XUV laser spectroscopy of atomic and molecular two-electron systems

W. Hogervorst[a], K.S.E. Eikema[b], E. Reinhold[a] and W. Ubachs[a]

[a]Laser Centre Vrije Universiteit, Department of Physics and Astronomy,
De Boelelaan 1081, 1081 HV Amsterdam, The Netherlands

[b]Present address: Max Planck Institute for Quantum Optics,
Hans Kopfermannstr. 1, D-85748 Garching, Germany

ABSTRACT

A tunable and narrowband extreme ultraviolet (XUV) laser source in the wavelength range of 100 - 50 nm has been applied to high resolution spectroscopy on the helium atom as well as on the hydrogen molecule. We excited the $1s^2\ ^1S_0$ -> $1s2p\ ^1P_1$ transition in He at 58.4 nm and measured the absolute transition frequency with a precision of better than $1{:}10^9$, allowing for a determination of the Lamb shift in the $1s^2\ ^1S_0$ ground state (41224(45) MHz) at the same level of accuracy as the theoretical value (41233 (35) MHz). In a two-step excitation process, involving a 91 nm XUV-photon and a visible photon, we populated vibrational and rotational states of the hydrogen molecule and its isotopomers in the outer part of a double-well potential. Long-lived states were observed in this potential at the large internuclear distance of 11 a.u. Complicated dynamical processes occur in the decay of these highly-excited states in H_2, D_2 and HD.

1. INTRODUCTION

The recent successful generation of narrowband and tunable extreme ultraviolet (XUV) laser radiation in our laboratory allows for high resolution spectroscopy of light atoms and molecules in the hitherto inaccessible wavelength range of 100 - 50 nm [1]. Within this wavelength range important excitation energies of the simplest two-electron helium atom and the lightest molecule H_2 can be found.

Progress in theoretical calculations of level energies make multi-electron atoms and ions of interest for studies of quantum electrodynamical (QED) effects. E.g. in helium and helium-like ions energy calculations without QED and higher-order relativistic effects are now so accurate that experimental transition frequencies can be used to deduce Lamb shifts. The self energy and vacuum polarization give the most important contributions to this Lamb shift. Helium is of particular interest because of two-electron contributions, arising from the mutual shielding of the nucleus by the electrons, decreasing the one-electron QED shift, and from a proximity effect of both electrons. The Lamb shift in the $1\ ^1S$ ground state as well as this two-electron contribution is more than an order of magnitude larger than in any excited state. Also isotope shifts ^4He - ^3He, containing important information on the difference in nuclear charge radii, in ground state

0375-9474/98/$19.00 © 1998 Elsevier Science B.V. All rights reserved.
PII S0375-9474(98)00033-5

transitions are largest. However, the ground state until recently was not easily accessible for laser excitation due to the large energy difference with excited states. In a preliminary experiment we demonstrated in 1993 that the 2 ^{1}P state could be excited from the 1 ^{1}S ground state using 58.4 nm laser radiation generated with a high power pulsed laser system and harmonic upconversion and that a value for the Lamb shift of the ground state could be extracted [2]. This feasibility study led us to start a dedicated, precision experiment on the 1 ^{1}S - 1 ^{1}P transition, of which results will be reported here.

The internuclear separation in diatomic molecules usually nearly equals the sum of the radii of the constituting atoms. Molecules in excited valence states for which the binding at the outer limb of the potential becomes ionic, such as in the B $^1\Sigma_u^+$state of the hydrogen molecule, show larger interatomic separations. Such states are represented by a single-minimum potential curve and their wave function density is at least partly concentrated at short distances. Double-well structures may result from avoided crossings between diabatic states with the same reflexion and inversion symmetry, multiplicity and orbital angular momentum. In H_2 a well-known example is the EF $^1\Sigma_g^+$ state with a second minimum at 4.4 atomic units (a.u.). In the potential of the fourth $^1\Sigma_g^+$ state in this molecule, called the $H\overline{H}$ state, a barrier and a second well are also formed. The outer well of $H\overline{H}$ is formed by the crossing of a repulsive H(1s) + H(2p) Heitler-London configuration with the $H^+ + H^-$ $(1s)^2$ ion-pair configuration. Its broad potential minimum is located at an internuclear separation as large as 11 a.u. and at an energy of 15 eV above the ground state, just 0.22 eV below the ionization threshold. Wolniewicz and Dressler performed ab initio calculations of the potential of the $H\overline{H}$ $^1\Sigma_g^+$ state and the energy levels of the various isotopes [3]. Recently we succeeded for the first time in the observation in H_2 of a series of long-lived vibrational-rotational levels in this outer well potential in a two-step laser excitation process involving one XUV photon and one visible photon [4]. Here we report some details of a study of these highly-excited levels in H_2, D_2 and HD, which show complicated dynamical processes in their decay.

2. EXPERIMENTAL SETUP

XUV radiation is generated using non-linear upconversion processes of tunable visible radiation from powerful pulsed laser systems. Firstly this light is frequency doubled in a non-linear KD*P crystal. Next the third and fifth harmonics of the UV light are produced in a dense, gaseous medium (C_2H_2, N_2 or Xe gas). Two versatile laser-based systems are operational in our laboratory. The first system operates with a moderate spectral resolution. We use a Quanta Ray pulsed tunable dye laser system with a Nd:YAG pump laser with a bandwidth of the order of 0.07 cm^{-1}, resulting in a XUV bandwidth of 0.2 cm^{-1} at 100 nm (third harmonics) and 0.3 cm^{-1} at 58 nm (fifth harmonics). The wavelength of the XUV radiation is calibrated on an absolute scale by monitoring the direct absorption spectrum of the visible light in a cell filled with I_2 molecules. Relative frequency measurements are performed with a Fabry-Perot interferometer. This system was used in the first experiments on the helium ground state [2] and in the first step of the excitation of the $H\overline{H}$ $^1\Sigma_g^+$ state in the hydrogen molecule [4] (see section 4).

In the second, high resolution system (see Fig. 1), we use an Ar^+- laser pumped CW ring dye laser (Spectra Physics) with a bandwidth of 1 MHz. The relative frequency of this radiation is measured with a high-finesse Fabry-Perot etalon and is again absolutely calibrated on I_2 lines. However, now we perform Doppler-free saturated absorption spectroscopy to achieve the high-

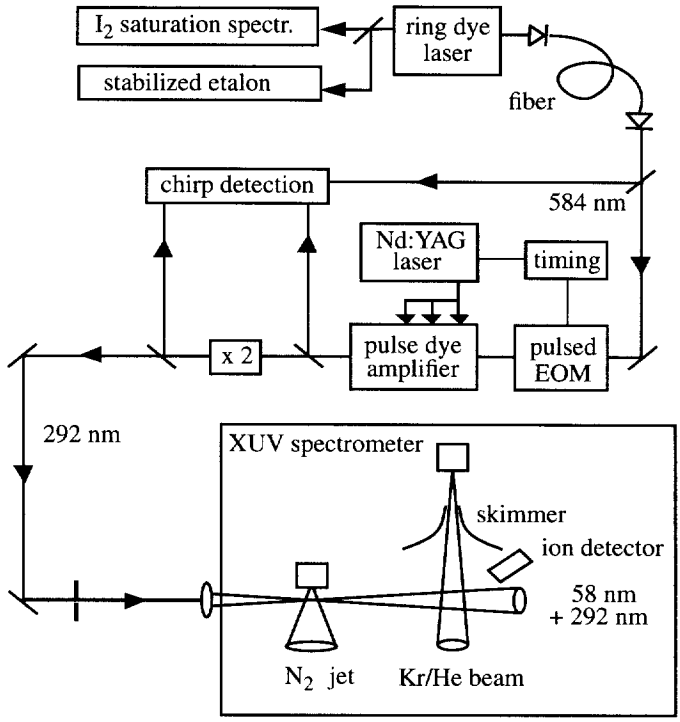

Figure 1. Schematic of the experimental setup for high precision XUV laser spectroscopy. The box in the lower right contains the vacuum setup for XUV generation and the interaction region with the He atomic beam. EOM: electro-optic modulator.

est precision. In a three-stage pulse-dye-amplifier (PDA), pumped by a powerful Nd:YAG laser (10 Hz, Quanta Ray), nearly Fourier-transform limited coherent radiation (bandwidth 85 MHz) is produced with a high pulse energy (200 mJ/pulse). This radiation can readily be upconverted to the UV and XUV [5,6]. With both systems of the order of 10^9 photons per pulse are generated in the third-harmonic process, about 10^5 photons in the fifth-harmonic process.

The frequency-doubled UV laser light is focused in a dense gas pulse to generate the harmonics. Since optically transparant window materials do not exist for radiation with a wavelength below 100 nm XUV photons are generated and transported inside a differentially-pumped vacuum system. Because of phase-matching conditions normally XUV- and UV-light propagate in the same direction (collinear). In some cases this is advantageous because of the possibility to use the copious amount of UV-photons to photoionize the atoms or molecules after their excitation with a XUV photon. This may facilitate signal detection. This was applied in the experiments on the helium atom. It is also possible to separate XUV and UV light in a non-collinear phase-matching configuration, such that no UV light is present in the excitation region. This configuration was used in the hydrogen experiment. In our experiments XUV and

UV laser light perpendicularly intersect a beam of atoms or molecules to be investigated, thus eliminating to a large extent Doppler broadening effects. Ions produced in a 1 XUV+1 UV photoionization process (in case of He) or in a multi-step scheme (in case of H_2) are extracted from the interaction region using pulsed electric fields and a time-of-flight setup for isotope-selective detection and are counted with an electron multiplier. Ion signals are stored on a computer as a function of the fundamental laser frequency, together with calibration signals from the I_2 molecule and the etalon.

3. QED IN THE HELIUM $1s^2\ ^1S_0$ GROUND STATE

With the narrowband source based on pulsed amplification of CW laser light at 584 nm we successfully excited the $1s^2\ ^1S_0$ -> $1s2p\ ^1P_1$ transition at 58.4 nm in He for both isotopes [5,6]. The frequency position of the resonance in the isotope ^{4}He in the XUV was accurately determined with respect to a hyperfine transition in I_2 in the visible, whereas the position of the ^{3}He resonance was accurately measured relative to that of ^{4}He using a well-calibrated high-finesse Fabry-Perot etalon. However, the extraction of precise values for the absolute transition frequency in ^{4}He as well as for the ^{4}He - ^{3}He isotope shift requires detailed assessment of possible sources of systematic errors. We identified, studied and eliminated three major error sources [6]. The first one is a possible Doppler shift due to non-perfect orthogonal alignment of atomic and XUV-laser beams. This effect, which may influence the absolute transition frequency but not the isotope shift, was investigated using a pure beam of He, where the atoms have a velocity of 1200 m/sec, and a beam seeded in krypton, where the He velocity drops to 500 m/sec. This procedure results in minor corrections, contributing 20 MHz to the error budget of the transition frequency. A second source relates to AC Stark shifts induced in the $1s2p\ ^1P_1$ upper state of the transition by the presence of the strong UV field. Its effect, which is isotope dependent because of the hyperfine structure of ^{3}He, could be assessed by varying the UV power and observing the shifts in the position of the ^{4}He resonance with respect to the I_2 calibration line. Extrapolation to zero field was straightforward and results in an error of 15 MHz in the transition frequency. From a calculation of the dynamical Stark effect in ^{3}He and ^{4}He it followed that the isotope shift has to be corrected by -6(3) MHz.

By far the most serious source of systematic errors is frequency chirp, which in particular may be severe in the amplification process of the CW laser light. Frequency excursions may result from phase variations induced by time-dependent, non-linear variations in the refractive index of the amplifying medium during pulsed irradiation. For this purpose we developed a system to measure and compensate frequency chirp effects on a pulse-to-pulse basis [6]. Firstly we measure a heterodyne beat signal between the amplified light and the CW laser light, which is shifted over 250 MHz with an acousto-optic modulator, recording simultaneously the shapes of the visible and frequency-doubled pulses on a fast digital oscilloscope. These signals contain sufficient information to extract shot-to-shot information on phase evolution and on frequency chirp. This information in turn is used to compensate chirp with a fast electro-optic modulator placed in the CW laser beam. The input phase of the CW beam is modified in such a way that phase distortions during the amplification process are counteracted, thereby eliminating frequency chirp to a negligible level during the time in which the XUV pulse is generated. After a careful and detailed study of all associated effects we quote a residual error due to frequency chirp effects of only 15 MHz.

An example of the ^{4}He resonance transition at 58.4 nm using anti-chirped PDA pulses, together with a saturated absorption spectrum of I_2 and an etalon spectrum, is shown in Fig. 2.

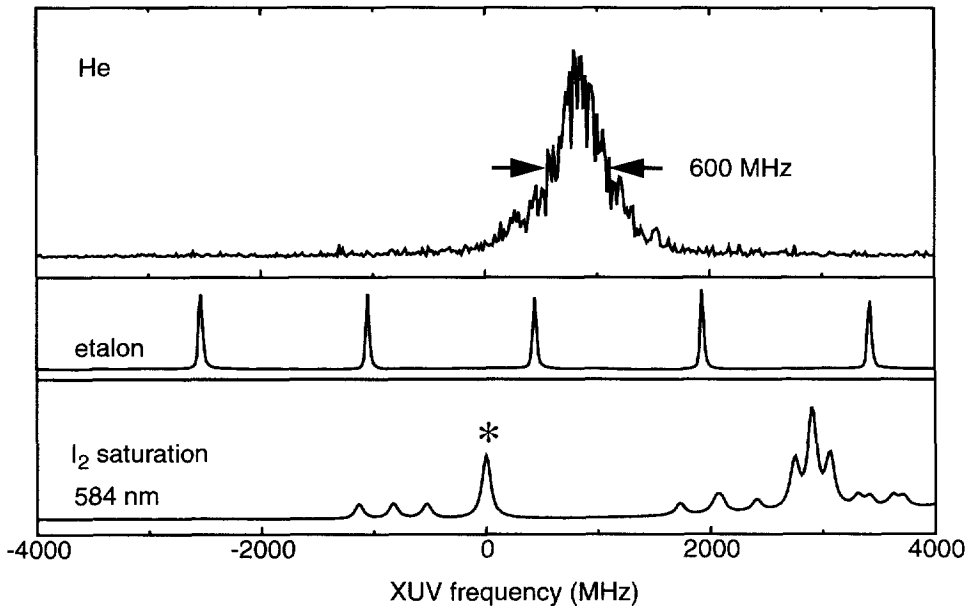

Figure 2. The 1 ^{1}S - 2 ^{1}P resonance transition in ^{4}He for anti-chirped PDA pulses with etalon and I_2 saturated absorption spectrum. The * indicates the "o"-component of the P88(15-1) transition used for absolute calibration.

The final result is an experimental ^{4}He transition frequency of 5130495083(45) MHz and an isotope shift ^{4}He - ^{3}He of 263410(7) MHz. These values compare well with theoretical results for the transition frequency of 5130495074(35) MHz and for the isotope shift of 263411.26(11) MHz [7,8]. The uncertainty in the calculation of the isotope shift only expresses the uncertainty in the knowledge of the difference in the nuclear radii of the ^{4}He and ^{3}He isotopes as QED effects in the transition frequencies are to a high degree equal for both isotopes. It shows that our experiment at its present level of accuracy is not sufficiently precise to improve existing values for this difference in nuclear radii.

The theoretical results on the transition energy of ^{4}He involve highly precise variational calculations of non-QED energy contributions as well as calculations of one- and two-electron QED contributions up to order (α^5Z^6) (one-electron) and order (α^4Z^4) (two-electron). The QED contributions are nearly equal in both isotopes and therefore cancel in the isotope shift. The theoretical error of 35 MHz in the absolute transition frequency relates to the uncertainty in the calculations of the one-electron terms of order $\alpha^4Z^5$and α^5Z^6. Both terms (contributing respectively 771.11 MHz and -68.8(35.) MHz to the theoretical value of the energy) are calcu-

lated assuming unscreened hydrogenic values with a correction for the electron density at the nucleus [8]. The 50% uncertainty in the latter contribution is an estimate. The excellent agreement between experiment and theory at the present level of accuracies shows the validity of this assumption. Subtracting the theoretical non-QED transition frequency from the experimental result and using the accurate theoretical value [8] for the Lamb shift of the $2\ ^1P$ state (37.5(1.8) MHz) results in an experimental value for the ground state Lamb shift of 41224(45) MHz. This has to be compared with the theoretical value 41233(35) MHz, which includes a one-electron contribution of 45440.9 (35) MHz and a two-electron effect of -4208 MHz. The size of this two-electron contribution is clearly confirmed in our experiment. Residual two-electron corrections of order $(\alpha^4 Z^4)$ remain to be calculated but are expected to contribute at the 10 MHz level to the shift of the $1\ ^1S$ ground state.

4. AN EXOTIC STATE IN THE HYDROGEN MOLECULE

With the XUV source based on the upconversion of light from a pulsed dye laser in combination with a visible laser we have excited vibrational and rotational states in the potential of the fourth $^1\Sigma_g^+$ state in the hydrogen molecule [4]. In this $H\overline{H}$-state an outer well is formed by the crossing of a repulsive H(1s) + H(2p) Heitler-London configuration with the $H^+ + H^-(1s)^2$ ion-pair configuration. The broad minimum of the outer-well potential is located at an internuclear separation as large as 11 a.u. and at an energy of about 15 eV above the ground state, only 0.22 eV below the ionization threshold (see left side Fig. 3). Only ab initio calculations [3] were available on this hitherto unobserved $\overline{H}$-state. For H_2 the outer well can sustain 16 vibrational levels below the top of the potential barrier (23 for D_2 levels and 18 for HD), part of which lie above the ionization threshold. For H_2 this is the case for the levels with v>4. However, for all but the highest of these states autoionization rates remain low because tunneling through a rather broad potential barrier is required to reach the internuclear distance of the electronic ground state of H_2^+ at the given energy. Also the predissociation process is predicted to have a small rate, so that the decay of these outer-well states is predominantly radiative with a predicted long lifetime of 140 nsec [3].

In a two-step excitation process we first selectively populate high ro-vibrational levels (v,J) of the B $^1\Sigma_u^+$ state with XUV radiation at 91.5 nm (λ_{xuv} in Fig. 3, right side). The UV light used to generate the XUV photons does not enter the interaction region with the hydrogen molecule. From these selected high-v levels of the B $^1\Sigma_u^+$ state the $\overline{H}$ levels, having appreciable Franck-Condon overlap at the outer limb of the B-state potential, are subsequently excited with tunable laser light in the range 556 - 735 nm (λ_{vis} in Fig. 3, right side). The visible and XUV laser pulses are counterpropagating and overlap in time in the interaction region. A third light pulse (either 355 nm from a Nd:YAG laser or tunable blue from a dye laser, λ_{uv} in Fig. 3, right side) is used to produce ions for probing the population of the $\overline{H}$-state. A variable time delay for the interaction with this third pulse and variation of its wavelength may be used to investigate the various dynamical decay processes. For this purpose we record in the time-of-flight detection setup separately the production of H_2^+ and H^+ ions, and their isotopes.

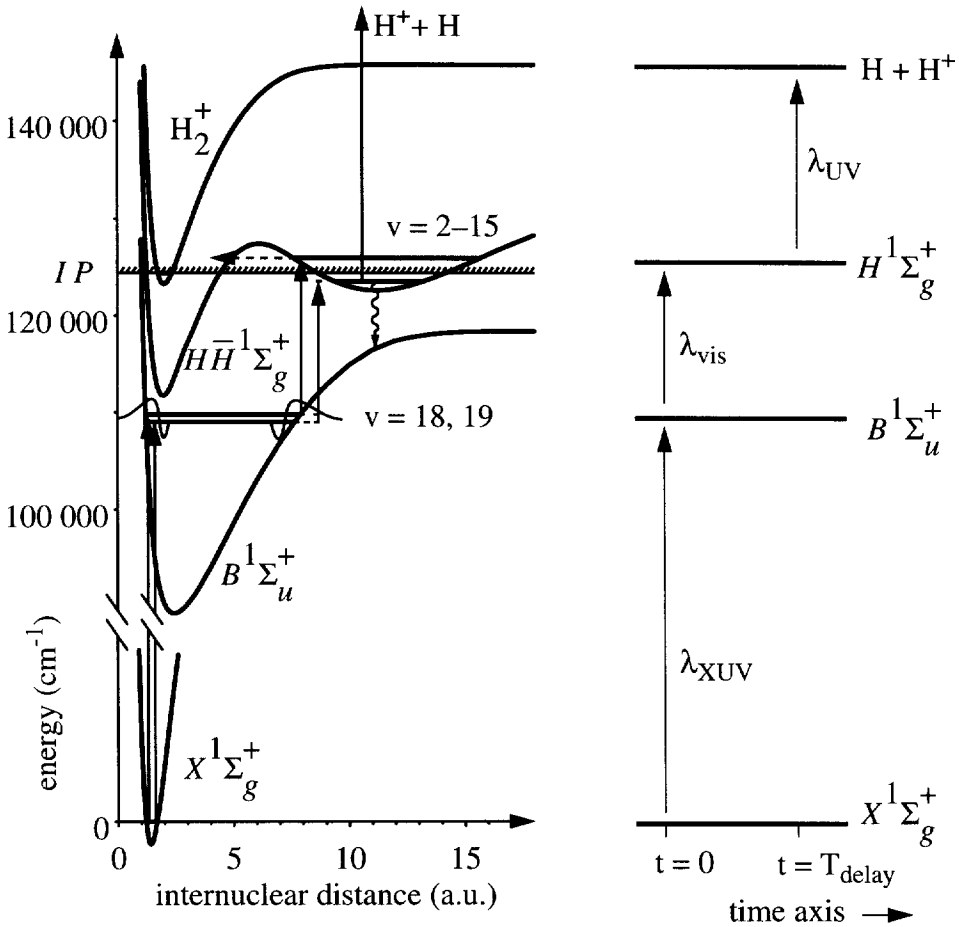

Figure 3. Potential energy curves of H_2 (left side) relevant for the two-step excitation with an XUV and a visible photon of rovibrational levels in the fourth $H\bar{H}\,^1\Sigma_g^+$ state (right side).With a third UV photon the population of the $H\bar{H}$ levels is probed, yielding H^+ ions for detection.

In the case of the homonuclear H_2 and D_2 molecule we have observed all but the few lowest vibrational states (14 out of 16 for H_2, 17 out of 23 for D_2). Rotational levels with J=0-5 have been investigated. As an example in Fig. 4 we show part of the spectrum of $\bar{H}\,^1\Sigma_g^+$ - $B\,^1\Sigma_u^+$ rovibrational transitions in D_2, using the v=27, J=2 intermediate state and recording the signal of D^+ produced by a delayed third UV pulse. It displays transitions to the v=9-13 vibrational $\bar{H}$ states with a spacing decreasing from about 209 cm^{-1} to 197 cm^{-1} and the characteristic dou-blet structure of a $^1\Sigma_g^+$ - $^1\Sigma_u^+$ transition with the P and R lines separated by 4.9 cm^{-1}.

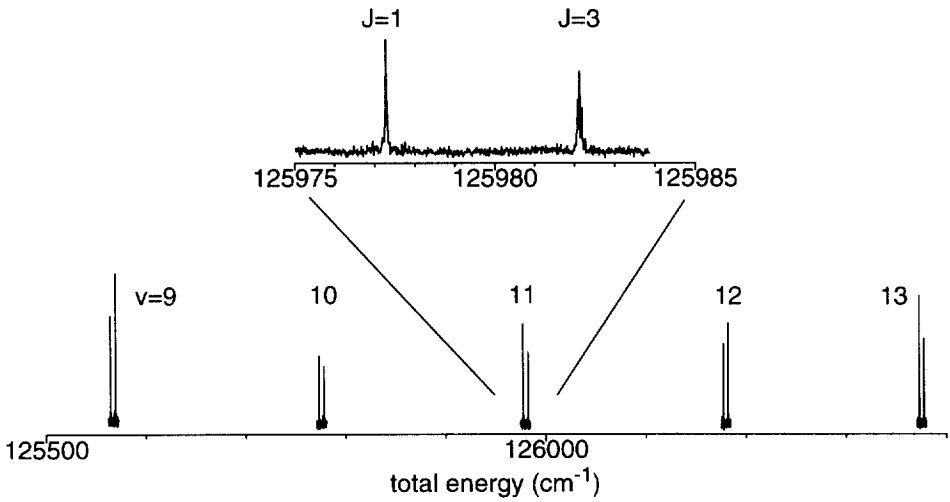

Figure 4. Spectrum of $\overline{H}^1\Sigma_g^+$ - B $^1\Sigma_u^+$ transitions in D_2, recorded from the v=27, J=2 intermediate state by scanning the second laser over the wavelength range 660-625 nm and detecting D^+ ions. P and R transitions to J=1 and J=3 are separated by about 4.9 cm^{-1}, as shown in the inset in higher resolution.

From a rotational analysis band origins and rotational constants could be derived for both H_2 and D_2, fitting the experimental energies with a rigid rotor relation. From the rotational constants for the various vibrational bands internuclear separations were deduced and found to decrease with increasing v, contrary to the behaviour in an anharmonic single-well potential. These internuclear separations for H_2 as a function of v are plotted in Fig. 5 as well as values calculated from vibrational wave functions [3].

The observed linewidths and the $H_2^+(D_2^+)$ and $H^+(D^+)$ signal strengths (as a function of the delay of the ionizing third pulse) contain relevant information on the decay dynamics. $H_2^+(D_2^+)$ is only detected, independent of the presence of the ionizing pulse, for the highest vibrational levels (v>11 for H_2, v>16 for D_2), which obviously do autoionize. This also follows from the observation of line broadening for these levels; the linewidth of lower levels does not exceed the laser linewidth of 0.06 cm^{-1}. $H^+(D^+)$ is not detected unless the ionizing radiation is present. These ions may be produced by transfer of population from the long-lived $\overline{H}$-state directly into the ionic dissociation continuum or by ionization of hydrogen atoms in the 2s state, populated in a predissociation process.

To investigate these decay channels in more detail we performed experiments varying both the wavelength of the ionizing pulse and T_{delay} (see Fig. 3) for levels with lower v-values, whereas for states with high v-values with linewidths exceeding the laser linewidth we directly measured this width. As an example we show in Fig. 6a the decay curve of the v=7, J=0 state, recorded by observing the H^+ yield as a function of the delay time of the ionizing pulse, for

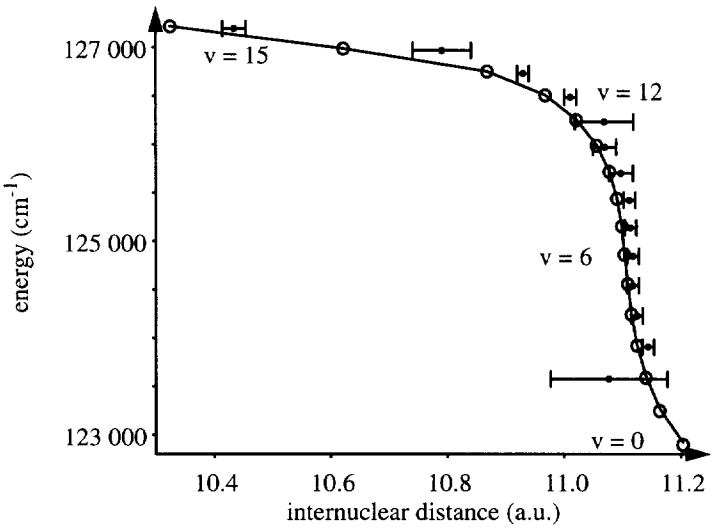

Figure 5. Mean internuclear separation for the outer-well vibrational $\overline{H}$ states of H_2 and a comparison with ab initio calculations of Wolniewicz and Dressler [3].

which in the case shown we used the third harmonic of a Nd:YAG laser at 355 nm. From this decay curve a lifetime for the v=7, J=0 $\overline{H}$ level in H_2 of 160 nsec is deduced. When we study the decay of this state with a longer wavelength (432 nm) pulse we observe a different decay time. With 432 nm radiation it is possible to ionize metastable H(2s) atoms produced by predissociation from the v=7 $\overline{H}$ level by tuning it on or off the Balmer γ-resonance. So these measurements in principle allow for a separation of the two dominant decay processes of radiative decay and predissociation. However, this separation is complicated by a worse s/n ratio in the 432 nm experiment than at 355 nm and by the fact that the predissocation product (H(2s) atoms) leave the detection zone with high kinetic energy, which hampers reliable measurements on lifetimes. In Fig. 6b we show a recording of the transition to the v=15 $\overline{H}$ level, which is the highest lying level in the outer potential well in case of H_2. It shows two strongly broadened rotational lines with J=1 and 3 with a linewidth of 1 cm^{-1}, corresponding to a lifetime of about 5 psec. In this case in the decay process also H_2^+ is formed as observed with the time-of-flight detector. Its formation does not depend on the presence of the ionizing UV radiation. H^+ signal is only detected, as in the case of the lower v-states, in the presence of the ionizing UV radiation. The strong reduction in lifetime and the production of H_2^+ ions demonstrates decay by rapid tunneling through the (low) barrier into the inner well of the $H\overline{H}^1\Sigma_g^+$ potential, from where rapid ionization occurs. The strong variation in H_2^+ peak heights in Fig. 6b may be due to resonant tunneling, when levels on either side of the potential well are sufficiently close, and to the branching ratio of the inner-well levels for autoionization and predissocation.

The case of the asymmetric HD molecule is even more complex. In addition to the excitation of the $H\overline{H}^1\Sigma_g^+$ state also the corresponding state with opposite inversion symmetry is excited

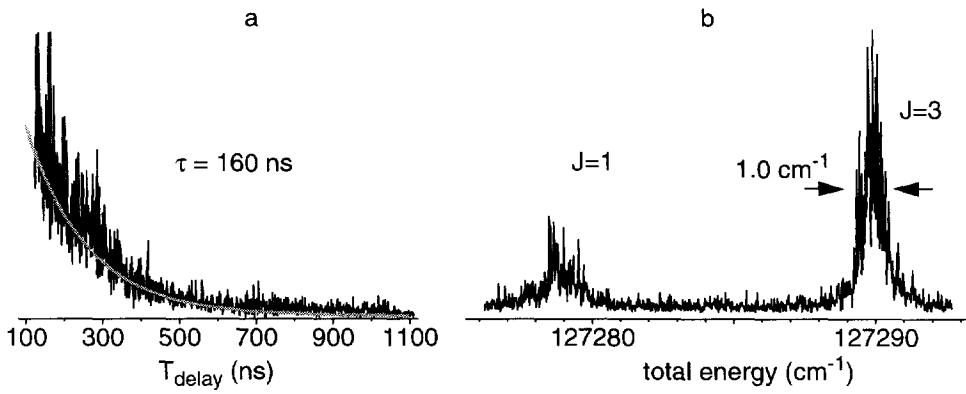

Figure 6. a. Decay of the v=7, J=0 $\overline{H}^1\Sigma_g^+$ level in H_2 studied by varying the time delay between the exciting pulses and the ionizing pulse at 355 nm. The H^+ ion yield is recorded.
b. Recording of the $\overline{H}^1\Sigma_g^+$ (v=15, J=1,3) - B $^1\Sigma_u^+$ (v=19, J=2) transitions in H_2. The large line-width and the observation of strong H_2^+ signals clearly demonstrate the tunneling from the outer to the inner well throuhg the barrier of the $H\overline{H}^1\Sigma_g^+$ potential.

(also at the level of the intermediate state), resulting in much more complicated excitation spectra and the opening of more decay channels. Detailed investigations of these features in HD are in progress.

ACKNOWLEDGEMENTS

The authors gratefully acknowledge financial support of the Vrije Universiteit (USF special grant) and the Foundation for Fundamental Research of Matter (FOM), which is part of the Netherlands Organization for the Advancement of Research (NWO).

REFERENCES

1. W. Ubachs, K.S.E. Eikema and W. Hogervorst, Appl. Phys. **B 57** (1993) 411.
2. K.S.E. Eikema, W. Ubachs, W. Vassen and W. Hogervorst, Phys. Rev. Lett. **71** (1993)1690.
3. L. Wolniewicz and K. Dressler, J. Chem. Phys. **100** (1994) 444 and references therein.
4. E. Reinhold, W. Hogervorst and W. Ubachs, Phys. Rev. Lett. **78** (1997)2543.
5. K.S.E. Eikema, W. Ubachs, W. Vassen and W. Hogervorst,Phys. Rev. Lett. **76** (1996)1216.
6. K.S.E. Eikema, W. Ubachs, W. Vassen and W. Hogervorst, Phys. Rev. **A 55** (1997) 1866.
7. G.W.F. Drake, I.B. Khirplovich, A.I. Milstein and A.S. Yelkhovsky, Phys. Rev. **A45** (1993) R15.
8. G.W.F. Drake, private communication.